HYDRODYNAMICS OF CUPRIC CHLORIDE HYDROLYSIS IN A FLUIDIZED BED FOR NUCLEAR HYDROGEN PRODUCTION

Y. Haseli, I. Dincer and G.F. Naterer
University of Ontario Institute of Technology, Oshawa, Ontario, Canada
E-mails: yousef.haseli@uoit.ca, ibrahim.dincer@uoit.ca, greg.naterer@uoit.ca

Abstract

The copper-chlorine (Cu-Cl) cycle has been identified by Atomic Energy of Canada Ltd. (AECL) as a promising cycle for thermochemical hydrogen production with a Super-Critical Water Reactor (SCWR). Currently a research group at the University of Ontario Institute of Technology (UOIT) is building an integrated laboratory demonstration of the Cu-Cl cycle for 5 kg H_2/day. This paper reports on the hydrodynamics of a reaction of cupric chloride particles with superheated steam in a fluidized bed reactor, as part of a Cu-Cl thermochemical cycle. Input heat to the cycle is supplied partly by waste heat for production of hydrogen, through splitting of water into oxygen and hydrogen. A numerical analysis is carried out to study the effects of the bed's operating parameters, such as the superficial gas velocity and bed inventory on bed height, average bubble diameter and bed void fraction. The results are presented for both a lab-scale and full-scale bed reactor. The consistency of the computed results is observed for both cases. When increasing the superficial velocity of the fluidizing gas (steam), it results in a taller bed height, larger mean bubble diameter and larger bed void fraction. Similar results are obtained with respect to the bed inventory. However, when it rises, the bed void fraction becomes smaller at a given gas velocity. Furthermore, it is shown that when the sphericity factor of the solid particles increases, the bed height decreases. These results provide useful new insight into the transport phenomena analysis of the reaction of copper chloride with steam.

1. Introduction

Currently the world consumes about 85 million barrels of oil and 104 trillion cubic feet of natural gas per day, releasing greenhouse gases that contribute to global warming. Unlike fossil fuels, hydrogen is a sustainable and clean energy carrier, which is widely believed to be the world's next-generation fuel. Hydrogen demand is expected to rise dramatically over the next few decades. The worldwide hydrogen market is currently valued at over 282 billion dollars per year, growing at 10%/year, doubling to 20%/year by 2010, and expected to continue rising to 40%/year by 2020 to reach several trillions dollars by 2020. Dincer [1] has outlined many of the key technical and environmental concerns of hydrogen production. The predominant existing process for large-scale hydrogen production is steam-methane reforming (SMR). However, SMR is a carbon-based technology that emits a primary greenhouse gas (carbon dioxide). In contrast, nuclear-based hydrogen production does not emit greenhouse gases. Nuclear heat can be supplied abundantly for large-scale capacities of hydrogen production [2]. Operating temperatures are key factors for thermochemical methods of hydrogen production. Thus, optimization of heat flows is important for high energy conversion efficiency [3]. Thermochemical "water splitting" requires an intermediate heat exchanger between the nuclear reactor and hydrogen plant, which transfers heat from the reactor coolant to the thermochemical cycle [4].

Atomic Energy of Canada Ltd. (AECL) [5] has identified the copper-chlorine (Cu-Cl) cycle to be a promising cycle for thermochemical hydrogen production. Water is decomposed into hydrogen and oxygen through intermediate Cu-Cl compounds. Currently a research team led by the University of Ontario Institute of Technology (UOIT) is building a laboratory demonstration of the Cu-Cl cycle for 5 kg H_2/day. Past studies of the copper-chlorine cycle may be found, for instance, in Refs. [2, 6-7]. The Cu-Cl thermochemical cycle uses a series of reactions to achieve the overall splitting of water into hydrogen and oxygen. The primary components of the cycle are four interconnected reaction vessels, with intermediate heat exchangers, and a drying step. The sequence of steps in the Cu-Cl cycle is shown in Table 1.

Table 1 - Steps in the Cu-Cl thermochemical cycle for hydrogen production [2]

Step	Reaction	Temperature Range, ^{0}C
1	$2Cu(s) + 2HCl(g) \rightarrow 2CuCl(l) + H_2(g)$	430-475
2	$2CuCl(s) \rightarrow 2CuCl(aq) \rightarrow CuCl_2(aq) + Cu(s)$	Ambient (electrolysis)
3	$CuCl_2(aq) \rightarrow CuCl_2(s)$	> 100
4	$2CuCl_2(s) + H_2O(g) \rightarrow CuO{*}CuCl_2(s) + 2HCl(g)$	400
5	$CuO{*}CuCl_2(s) \rightarrow 2CuCl(l) + 1/2O_2(g)$	500

This paper focuses on reaction 4 in Table 1 of the Cu-Cl cycle, when cupric chloride particles are brought to react with superheated steam in a fluidized bed reactor. The purpose is to study the hydrodynamic behavior of the reaction, leading to better understanding of the interaction between key bed properties, such as the superficial velocity, bed inventory, bed height, void fraction, etc. The reaction of cupric chloride particles with steam is an endothermic reaction that requires a certain amount of heat input, depending upon the reaction temperature. Figure 1 depicts the Gibbs energy of this reaction, as a function of temperature. At 375^{0}C, the value of ΔG (31.6 kJ/mole) given by Lewis [8] is close to the computed value in this paper.

This paper is primarily intended to study the fluid-dynamics of the fluidized bed reactor, as a basis for future studies on transport phenomena of the step 4 reaction. A solution algorithm is introduced in this paper to enable a numerical investigation on hydrodynamics of the bed. Moreover, the results are presented both for a lab-scale and full-scale reactor.

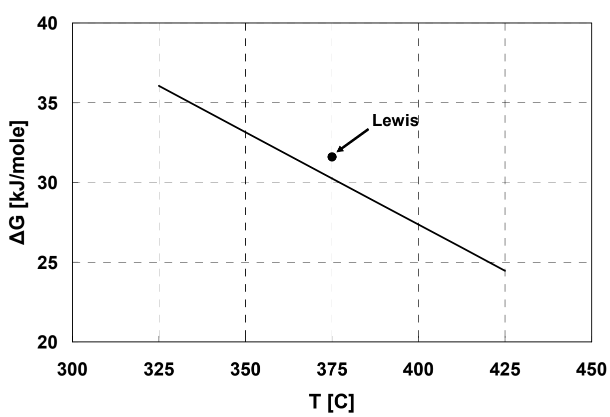

Figure 1 - Gibbs free energy for the reaction of cupric chloride particles with steam at various reaction temperatures. The marker in the figure is a value given by Lewis [9].

2. Hydrodynamics of the fluidized bed

This section analyzes the hydrodynamics of a fluidized bed reactor which is schematically shown in Fig. 2. The governing equations can be used to evaluate bed properties and determine the key parameters related to the fluid-dynamics of gas-solid mixing phenomena, within a fluidized reactor.

2.1 Bubble velocity

The minimum fluidization velocity as described by Grace [9] is determined from Eq. (1) for $Ar<10^3$.

$$U_{mf} = 0.00061 \frac{g(\rho_p - \rho_g) d_p^2}{\mu_g} \tag{1}$$

Equation (1) shows the influence of key variables on U_{mf}. For group B particles (cupric chloride particles in this study), the bubbling begins as soon as the superficial velocity of the gas exceeds U_{mf}, so that the minimum bubbling velocity, U_{mb}, is equal to U_{mf}.

For Geldart B solids, the velocity of a bubble is defined as [10]

$$U_b = 1.6\left[\left(U_o - U_{mf}\right) + 1.13 d_b^{0.5}\right] D_t^{1.35} + U_{br} \tag{2}$$

where d_b denotes the bubble diameter, D_t is the bed diameter and U_{br} represents the relative velocity of the bubble, defined as

$$U_{br} = 0.711 (g.d_b)^{0.5} \tag{3}$$

2.2 Void fraction (bed void fraction)

The bed void fraction represented by ε_b is another important parameter of a fluidized bed. The following expression [11] is utilized to determine this parameter.

$$\varepsilon_b = 1 - \frac{1 - \varepsilon_{mf}}{1 + \dfrac{U_o - U_{mf}}{U_{br}}} \tag{4}$$

where ε_{mf} represents the bed void fraction at minimum fluidization conditions, which are usually defined based on experimental measurements. However, if there is a lack of data, it may be estimated based on the particle spherecity, ϕ_s as

$$\varepsilon_{mf} = \left(\frac{1}{14\phi_s}\right)^{1/3} \tag{5}$$

2.3 Bed height

It is essential to first present the expression which describes the bed height at minimum fluidization as follows,

$$L_{mf} = \frac{W_b}{\rho_p (1-\varepsilon_{mf})(\pi D_t^2 / 4)} \tag{6}$$

where W_b is the bed inventory. Thus, one may obtain the bed height at an operating condition of the fluidized bed using Eq. (7) [10].

$$L_f = L_{mf} \frac{1-\varepsilon_{mf}}{1-\varepsilon_b} \tag{7}$$

2.4 Bubble diameter

The local bubble diameter at a given height above the distributor (z) can be calculated as

$$d_b = d_{bm} - (d_{bm} - d_{b0}) exp\left(-0.3 \frac{L_f}{D_t} z\right) \tag{8}$$

where d_{bm} and d_0 denote, respectively, the maximum and initial bubble diameters defined as

$$d_{bm} = Min\left\{163.77\left[0.7854.(U_o - U_{mf}).D_t^2\right]^{0.4}, D_t\right\} \tag{9}$$

$$d_{b0} = \begin{cases} \dfrac{0.082}{g^{0.2}}\left[\dfrac{U_o - U_{mf}}{N_{or}}\right]^{0.4} & d_{b0} \le l_{or} \\ \dfrac{0.0278}{g}(U_o - U_{mf})^2 & d_{b0} > l_{or} \end{cases} \tag{10}$$

Here N_{or} represents the holes density of the distributor, and l_{or} denotes the holes pitch on the distributor. The average bubble diameter throughout the bed can be defined by integrating Eq. (8) along the bed height as follows,

$$d_{b,ave} = \frac{1}{L_f}\int_0^{L_f} d_b dz \tag{11}$$

The solution of the above integration, taking into consideration Eq. (7), yields

$$d_{b,ave} = d_{bm} + \left(\frac{D_t}{0.3L_f^2}\right)(d_{bm} - d_{b0})\left[exp\left(-0.3\frac{L_f^2}{D_t}\right) - 1\right] \tag{12}$$

2.5 Solution procedure

In order to analyse the transport phenomena of the fluidized bed, detailed understanding of the fluid-dynamic properties of the bed is essential. It is first needed to evaluate the bed height, average values of the bubble diameter, bed voidage, etc. A solution flowchart is then developed for determining the bed height, bed voidage and average bubble diameter, as illustrated in Fig. 3. This flowchart has been employed in this paper to study the hydrodynamics of a lab-scale bed and a full-scale bed.

3. Results and Discussion

The hydrodynamic analysis of fluidized beds in the preceding section is used to investigate fluid-dynamics of the reaction of cupric chloride particles with superheated steam. The influence of the superficial velocity and bed inventory on bed height, bed void fraction and average bubble diameter are studied for two bed scales: lab (bench) scale bed, and full-scale bed.

3.1 Lab-scale bed results

Figure 4 shows the variation of bed height, average bubble diameter and bed voidage versus superficial velocity at three various values of bed inventory. The bed is 16.5-cm high and it has a diameter of 2.66-cm. Increasing the superficial velocity results in a higher bed height, since the upward force of the gas stream acting on suspended particles increases. As expected, the bed height is higher at larger bed inventories (Fig. 4a). The predicted average bubble diameter versus superficial velocity of the gas is shown in Fig. 4b. At a low flow rate of steam, the initial bubbles formed above the distributor are not big enough to contact each other. In contrast, when the gas flow rate is high, the initial bubbles are big enough so they overlap when formed. As observed in Fig. 4b, a higher velocity (steam flow rate) results in larger bubbles. On the other hand, Fig. 4b shows that the bubble average diameter is larger at a heavier bed inventory. This may be due to a taller bed height at a larger bed inventory, so that neighboring bubbles have more opportunity to contact and form larger bubbles, which on average would lead to a larger bubble diameter at a heavier inventory. Furthermore, Fig. 4c shows that a higher superficial velocity may cause a larger bed void fraction. This occurs since a high flow rate of gas at a specific bed geometry would occupy more volume of the bed, thereby leading to higher void fraction of the bed. However, at a certain gas velocity, the bed void fraction can be reduced by increasing the bed inventory, which would require more space.

The effect of particle diameter in the range of 0.15-35 mm is also investigated. The outcome is depicted in Fig. 5, in terms of bed height at varying superficial velocities. A higher bed height for smaller particles occurs, since with the same amount of bed inventory, smaller particles lead to a larger gap-space between adjacent particles, which may cause a taller bed height.

Figure 6 illustrates the influence of particle sphericity on the bed height at three different bed inventories. As the particle shape becomes more spherical, the height of the bed decreases. When the particles have an irregular shape, there will be more free space between adjacent particles, compared to the situation when the particles are closer to a spherical shape. Hence, when the particle sphericity is smaller, the bed height at a given bed inventory would be taller.

Lastly, the pressure drop in the stream of steam flowing through the cupric chloride particles in the bed is further calculated as a function of bed inventory. The results are represented in Fig. 7. It can be observed that a heavier inventory would cause more resistance against the path of gas flow and the pressure of the gas stream would reduce more.

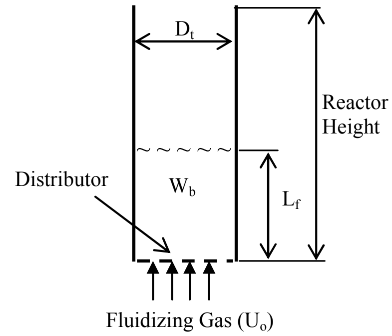

Figure 2 - Schematic diagram of fluidized bed reactor

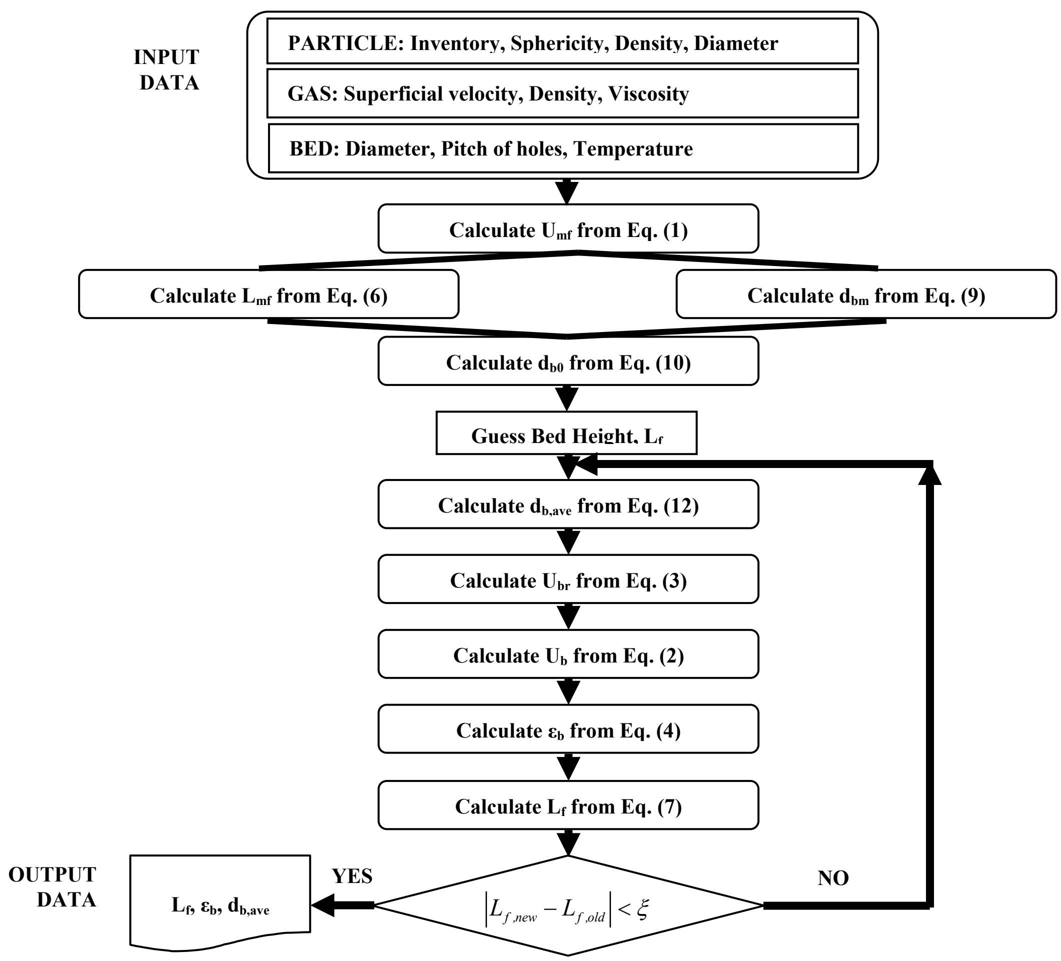

Figure 3 - Solution flowchart for evaluating the bed properties

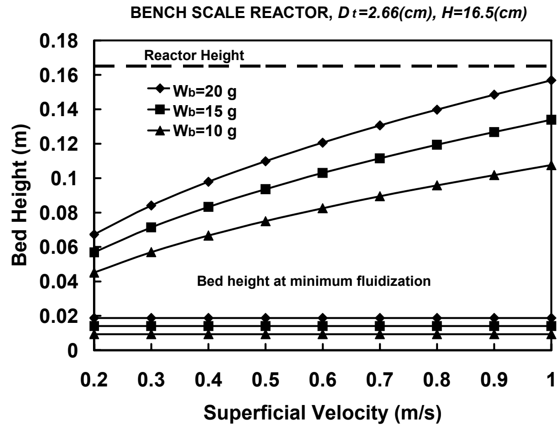

(a)

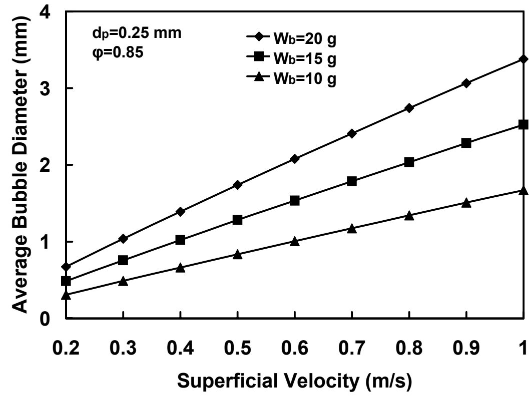

(b)

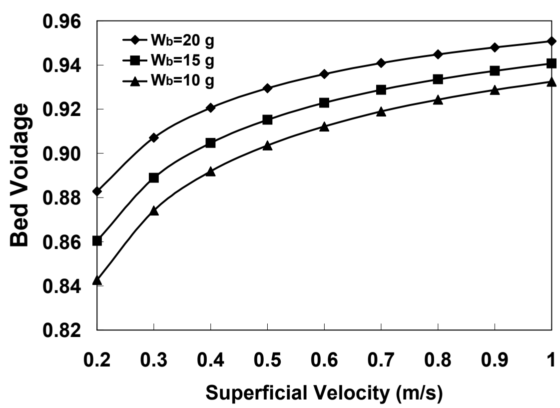

(c)

Figure 4 - Effects of superficial velocity on (a) Bed height, (b) Average bubble diameter, and (c) Bed voidage, at different inventories

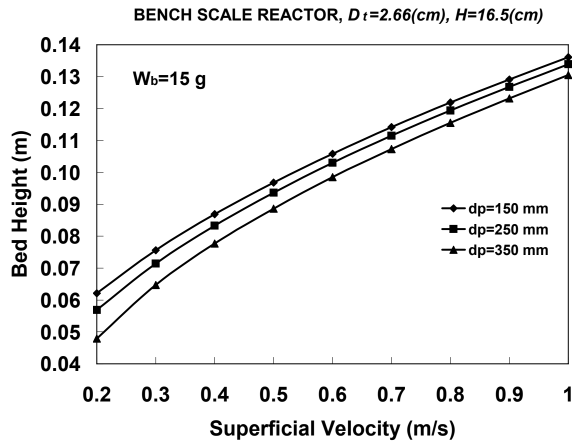

Figure 5 - The effect of particle diameter on bed height

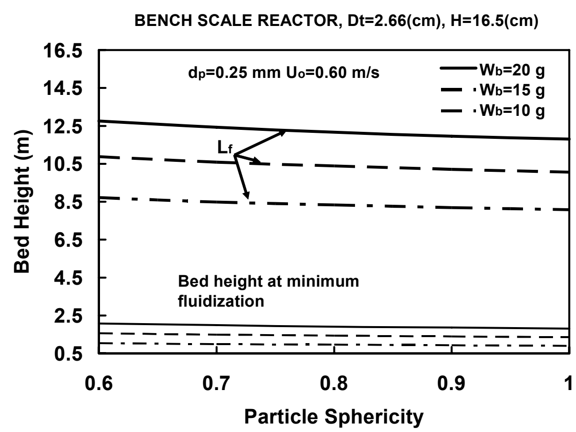

Figure 6 - The effect of particle sphericity on bed height

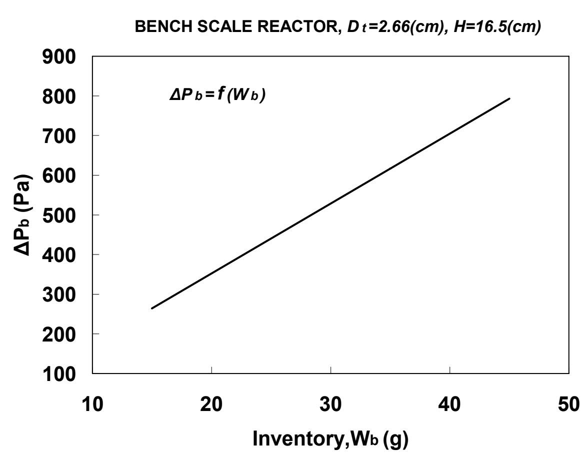

Figure 7 - Pressure drop along the bed versus bed inventory

3.2 Full-scale bed results

In order to investigate the consistency of the hydrodynamic analysis described in section 2, it is important to observe the hydrodynamic behavior of a commercial unit. Considering a scaling factor, m=24 (as an example), compared to the lab-scale reactor of section 3.1, the height and diameter of the reactor are assigned, respectively, as 4m and 0.6448m. Likewise, the effects of gas velocity, bed inventory and particle sphericity on bed height, average bubble diameter and bed voidage are studied. The results are depicted in Figs. 8-9. The predicted results for a full-scale reactor in Fig. 8 are qualitatively the same as the graphs of Fig. 4. Similarly, increasing the superficial velocity causes an increase in bed height, average bubble diameter and bed void fraction. Also, a heavier bed inventory may result in a taller bed height and larger bubble diameter, whereas it can lead to a smaller bed void fraction.

Additionally, Fig. 9 illustrates the variation of bed height versus particle sphericity in a full-scale bed, at three different values of inventory. On an average basis, when the sphericity increases from 0.6 to 1.0, the bed height decreases 11.8% and the bed height at a minimum fluidization reduces by 13.2%. These values for lab-scale results (Fig. 6) are 7.5% and 12.8%, respectively, for the bed height and minimum fluidization bed height at W_b=15 g.

Figure 10 shows the pressure drop in the fluidizing gas stream in the range of 500-1500 kg inventory. It is observed that in a commercial reactor, the pressure drop throughout the bed is an important issue compared to the lab scale (Fig. 7).

4. Conclusions

A research effort is being undertaken at the University of Ontario Institute of Technology (UOIT) to build a laboratory prototype for hydrogen production using a thermochemical copper-chlorine (Cu-Cl) cycle, which includes 5 steps of reactions. Results on the hydrodynamic behavior of step 4 in the Cu-Cl cycle, which includes a reaction of cupric chloride particles with superheated steam, are reported in this paper. Understanding the hydrodynamics of the reaction is essential in ongoing research on transport phenomena of the thermochemical reaction that takes place in a fluidized bed reactor.

The analysis is applicable for either a lab-scale or full-scale bed reactor to observe the effects of various key parameters, e.g. superficial gas velocity, bed inventory, particle sphericity, etc. on bed behaviour. Overall, consistent results are achieved for the hydrodynamics of both a lab-scale and full-scale bed. The numerical results indicate that the bed height, average bubble diameter and bed voidage may increase with the superficial velocity. On the other hand, increasing the bed inventory is seen to cause an increase in bed height and bubble diameter, while it may result in a smaller bed void fraction. These outcomes explicitly show under which situation the bed entrainment might occur.

5. Acknowledgments

The authors acknowledge the support provided by Atomic Energy of Canada Limited and the Ontario Research Excellence Fund.

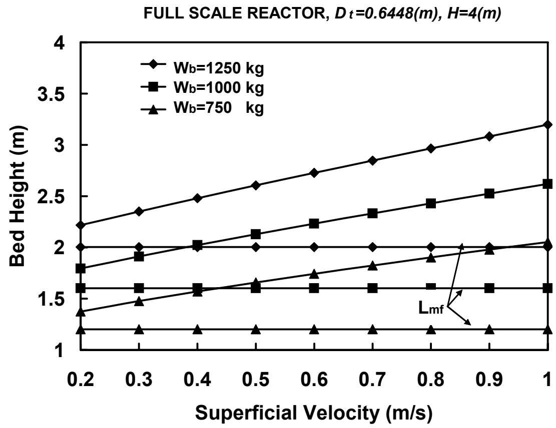

(a)

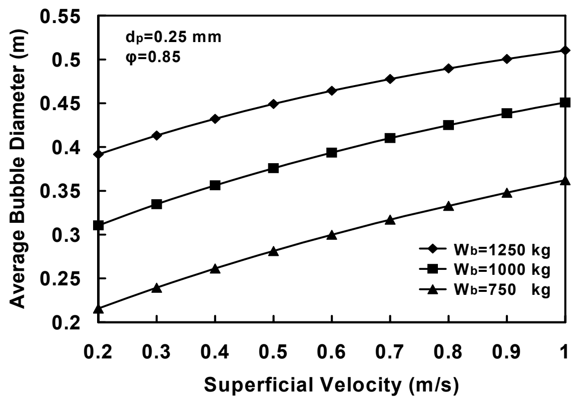

(b)

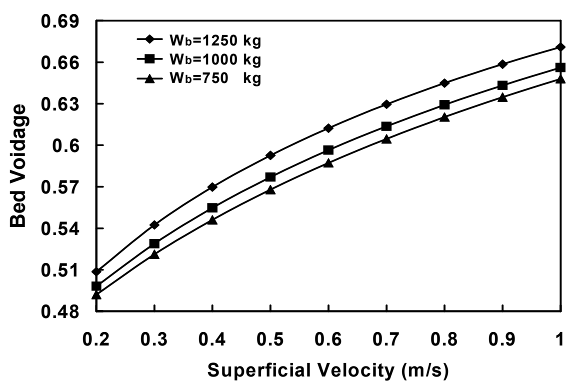

(c)

Figure 8 - Effects of superficial velocity on (a) Bed height, (b) Average bubble diameter, and (c) Bed voidage, at different inventories (Full-Scale Bed)

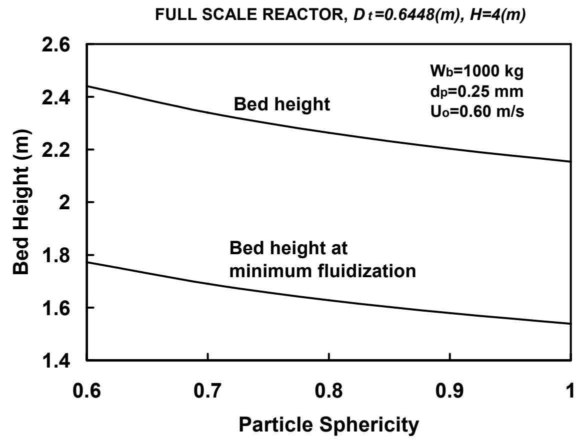

Figure 9 - The effect of particle sphericity on bed height (Full-Scale Bed)

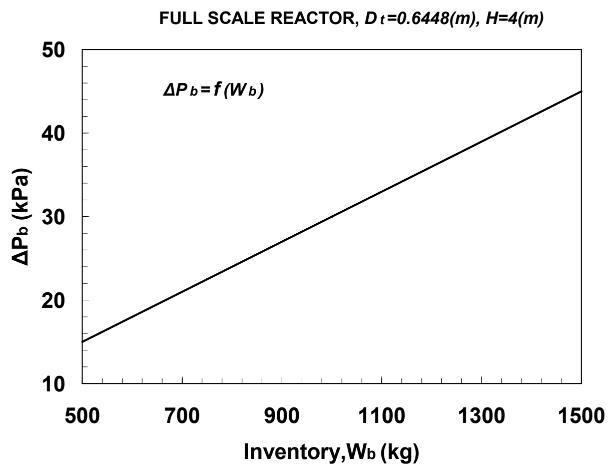

Figure 10 - Pressure drop along the bed versus bed inventory (Full-Scale Bed)

Nomenclature

Ar	Archimedes number
d_b	bubble diameter, m
d_{b0}	initial bubble diameter, m
$d_{b,ave}$	average bubble diameter, m
d_{bm}	maximum bubble diameter, m
d_p	particle mean diameter, m
D_t	bed diameter, m
g	acceleration of gravity, 9.81m/s
l_{or}	spacing between adjacent holes on the distributor, m
L_f	bed height, m
L_{mf}	bed height at minimum fluidization conditions, m
N_{or}	hole density of the distributor, m^{-2}
U_o	superficial velocity, m/s

U_b	velocity of bubble, m/s
U_{br}	relative velocity of bubble, m/s
U_{mf}	minimum fluidized velocity, m/s
W_b	bed inventory, kg

Greek letters

ε_b	bed void fraction (voidage)
ε_{mf}	bed void fraction at minimum fluidization conditions
μ_g	gas viscosity, Pa/s
ρ_g	gas density, kgm^{-3}
ρ_p	particle density, kgm^{-3}
ϕ_s	particle sphericity

References

[1] Dincer I., "Technical, Environmental and Exergetic Aspects of Hydrogen Energy Systems", *International Journal of Hydrogen Energy*, vol. 27, no. 3, 2002, pp. 265-285.

[2] Rosen M. A., Naterer G. F., Sadhankar R., Suppiah S., "Nuclear-based hydrogen production with a thermochemical copper-chlorine cycle and supercritical water reactor", *Canadian Hydrogen Association Workshop*, Quebec, October 19 - 20, 2006.

[3] Naterer G. F., *Heat Transfer in Single and Multiphase Systems*, CRC Press, Boca Raton, FL, 2002.

[4] Forsberg C. W., “Hydrogen, Nuclear Energy and Advanced High-Temperature Reactor”, *International Journal of Hydrogen Energy*, vol. 28, 2003, pp. 1073-1081.

[5] Sadhankar R. R., Li, J, Li, H., Ryland, D. K., Suppiah, S. “Future Hydrogen Production Using Nuclear Reactors”, *Engineering Institute of Canada – Climate Change Technology Conference*, Ottawa, May, 2006.

[6] Serban M., Lewis M. A., Basco J. K., “Kinetic study of the hydrogen and oxygen production reactions in the copper-chloride thermochemical cycle”, *AIChE 2004 Spring National Meeting, New Orleans*, LA, April 25-29, 2004.

[7] Lewis M. A., Masin J. G., Vilim R. B., “Development of the low temperature Cu-Cl thermochemical cycle”, *International Congress on Advances in Nuclear Power Plants*, Seoul, Korea, May 15-19, 2005.

[8] Lewis M. “Recent advances in the Cu-Cl cycle’s developments at Argon National Laboratory”, *Workshop on Thermochemical Nuclear-Based Hydrogen Production*, UOIT, Oshawa, Ontario, Canada, May 28, 2007.

[9] Crowe T. C., “Multiphase flow handbook”, CRC Press, Boca Raton, FL, 2006, Chap. 5.

[10] Kunii D., Levenspiel O., “Fluidization Engineering”, 2nd edition. Butterworth-Heinemann, London, 1991.

[11] Thompson M. L., Bi H., Grace J. R., “A generalized bubbling/turbulent fluidized-bed reactor model“, *Chemical Engineering Science* vol. 54, 1999, pp. 2175-2185.